Improved Physical Layer Implementation of VANETs

Latif Ullah Khan, M. Irfan Khattak, Naeem Khan, Atif Sardar Khan, and M. Shafi

Department of Electrical Engineering, University of Engineering & Technology/ Peshawar, Pakistan
  latifullahkhan@nwfpuet.edu.pk

* Corresponding Author: Latif Ullah Khan

* Regular Paper

Abstract: Vehicular Ad-hoc Networks (VANETs) are comprised of wireless mobile nodes characterized by a randomly changing topology, high mobility, availability of geographic position, and fewer power constraints. Orthogonal Frequency Division Multiplexing (OFDM) is a promising candidate for the physical layer of VANET because of the inherent characteristics of the spectral efficiency and robustness to channel impairments. The susceptibility of OFDM to Inter-Carrier Interference (ICI) is a challenging issue. The high mobility of nodes in VANET causes higher Doppler shifts, which results in ICI in the OFDM system. In this paper, a frequency domain comb-type channel estimation was used to cancel out ICI. The channel frequency response at the pilot tones was estimated using a Least Square (LS) estimator. An efficient interpolation technique is required to estimate the channel at the data tones with low interpolation error. This paper proposes a robust interpolation technique to estimate the channel frequency response at the data subcarriers. The channel induced noise tended to degrade the Bit Error Rate (BER) performance of the system. Parallel concatenated Convolutional codes were used for error correction. At the decoding end, different decoding algorithms were considered for the component decoders of the iterative Turbo decoder. A performance and complexity comparison among the various decoding algorithms was also carried out.

Keywords: OFDM, Comb-type channel estimation, Low pass interpolation, ICI, LS estimator

1. Introduction

Vehicular Adhoc Networks (VANETs) are a special kind of Mobile Adhoc Network (MANET) comprised mainly of vehicular nodes with high mobility and more power resources compared to the typical MANET node [1]. Orthogonal Frequency Division Multiplexing (OFDM) is an excellent candidate for communication at the physical layer of VANETs. Wi-Fi, Wi-Max, power line communications, ADSL, Digital Video broadcasting (DVB) and Digital Audio Broadcasting (DAB) use OFDM for Communication because of its inherent spectral efficiency feature [2, 3]. The spectral efficiency of OFDM is due to the overlapping nature of the orthogonal subcarriers. The effect of Inter-Symbol Interference (ISI) introduced by a multipath fading channel in single carrier communication systems is mitigated through the use of complex equalization techniques. In OFDM, however, ISI is cancelled out simply through the use of a guard interval [4]. The sensitivity of OFDM to frequency and time

synchronization errors are its major disadvantages. Frequency offset errors occur due to high Doppler shifts. Frequency offset errors disturb the alignment of the orthogonal subcarriers and cause ICI.

In the literature, various approaches have been used for ICI cancellation. In [5], ICI was mitigated by the application of multi-rate sampling theory to the OFDM symbol. The sequential interference cancellation detection scheme is based on the supposition of a perfect channel estimation. The detection scheme first detects the data from the outer subcarriers. The interference induced on the inner subcarriers by the already detected outer subcarriers is cancelled out first, and the signal form the inner subcarriers is then detected. The sequential fashion of detection is from the outer subcarriers to the inner subcarriers. The proposed ICI cancellation algorithm has the disadvantage of high computational complexity. Jianhua *et al* in [6] proposed an ICI self-cancellation technique to cancel out the ICI caused by phase noise. The ICI self-cancellation scheme introduces redundancies to

protect the OFDM symbol. On the other hand, the proposed self ICI cancellation scheme has the disadvantage of spectral inefficiency because only half of the subcarriers are used for data. Seyedi *et al* in [7] proposed a general ICI self-cancellation scheme. This scheme was implemented using windowing at the receiver and transmitter. The proposed general self ICI cancellation technique has low computational complexity and performs well in the presence of ICI generated because of the oscillator frequency offsets and fast fading channel but at the cost bandwidth inefficiency.

The two-stage equalizer for ICI cancellation proposed by Hou *et al* in [8] is based on the assumption of a linear variation of the channel frequency response during the block period of time. This technique is comprised of a set of pre-filters and ICI cancellation filters. The multiplicative distortion is mitigated through pre-filters and the ICI is cancelled out by the second set of filters. The downside of the proposed ICI cancellation scheme is the assumption of a linear channel impulse response over a block period of time. The channel impulse response varies rapidly over time for fast fading channels. Therefore, the proposed two stage equalizer is undesirable for a fast fading channel.

Berrou *et al* [9] first presented the idea of Turbo codes. Turbo codes are powerful error correction codes adopted in many wireless communication standards i.e. DVB-RCS, 3GPP UMTS and IEEE 802.11 [10]. The reason for considering Turbo codes in OFDM for VANETs is their powerful error correction capability. Turbo codes can be constructed from linear block codes or convolutional codes concatenated serially or in a parallel manner. In 802.11p-based vehicular networks, only convolutional codes were proposed for error correction. On the other hand, the performance of turbo codes is better than Reed Solomon and Convolutional codes [11]. This is why Turbo codes were used in this paper.

In this paper, a comb-type channel estimation was employed to eliminate ICI. The channel impulse response was estimated at pilot tones using a Least Square (LS) estimator. An efficient interpolation technique was proposed to estimate the channel frequency response at the data tones. The performance of the proposed interpolation technique was compared with other one-dimensional interpolation techniques including low pass, spline and linear interpolation. This is because the channel induced noise degrades the BER performance of the OFDM system. This paper proposes the use of Turbo codes for error correction. Parallel concatenated Convolutional codes were considered for error correction. At the decoding side, an iterative Turbo decoder consisting of two component decoders was employed. Different decoding algorithms, namely the Maximum A *Posteriori* (MAP) Algorithm, Log-MAP, and Max-Log-MAP algorithms, were considered for the component decoders. The component decoder exchanges soft information in different iterations to improve the performance of the iterative Turbo decoder. A performance comparison and complexity comparison among the component decoding algorithms was also made. The effect of a change in memory order on the performance of the decoding algorithms is also studied.

The remainder of the paper is structured as follows. Section II provides an overview of the proposed system model. The anatomy of the iterative Turbo decoder and encoder are discussed in Section III. The turbo decoding algorithms for the component decoders are explained in Section IV. The proposed ICI cancellation algorithm with mathematical manipulation is outlined in Section V. Simulation results and analysis is discussed in Section VI. Paper is concluded in Section VII.

Notation: $(\ )^H$ and $(\ )^T$ represent the Hertmitian transposition and transposition, respectively. The vectors and matrices are represented by bold face lower case italics letters and bold face upper case italics letters, respectively.

2. OFDM System Model

In the OFDM System illustrated in Fig. 1, the input bits are first encoded and then mapped to produce the frequency domain sequence of symbols. A description of the encoder is given in the subsequent section. The mapped sequence of the frequency domain symbols is divided into groups of size $N_d = N - N_p$ (where N = total number of subcarriers and N_p = subcarriers reserved for pilots per OFDM symbol) equal to the number of subcarriers reserved for data per OFDM symbol. The ith OFDM symbol is $\boldsymbol{d}^{(i)} = [\, d^{(i)}(0),\, d^{(i)}(1), ...,\, d^{(i)}(N_d - 1)]^T$. The serial sequence of the symbols is parallelized and the pilot symbols are then inserted at the dedicated subcarriers. The resulting frequency domain parallelized sequence is converted to a time domain sequence $\boldsymbol{s}^{(i)} = [\, s^{(i)}(0),\, s^{(i)}(1), ...,\, s^{(i)}(N - 1)]^T$ through the operation of IDFT.

$$\boldsymbol{s}^{(i)} = \boldsymbol{F}\, \boldsymbol{d}^{(i)} \qquad (1)$$

where $[\boldsymbol{F}]_{n,m} = \frac{1}{\sqrt{N}} e^{j2\pi(m-1)(n-1)/N}$ for $n = 0, 1, 2, …, N-1$ and $m = 0, 1, 2, …, N-1$. Inter-Symbol Interference is caused by the multipath fading channel effect. A cyclic prefix is added by inserting the last L_G symbols at the start of the OFDM symbol for an ISI cancellation. The length of L_G must be kept greater than or equal to the channel order (Length of the channel) for effective cancellation of ISI. The signal, after inserting the cyclic prefix is $\boldsymbol{s_{CP}}^{(i)} = [s_{CP}^{(i)}(-L_G + N), s_{CP}^{(i)}(-L_G + N + 1),$
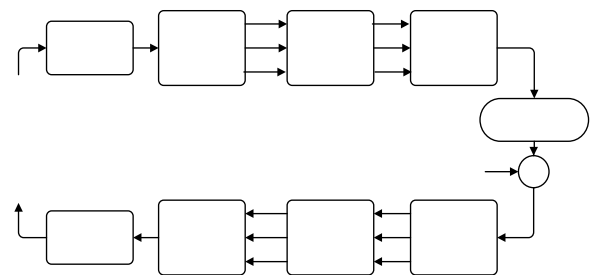

Fig. 1. OFDM System Model.

..., $s_{CP}^{(i)}((N-1))$, $s_{CP}^{(i)}(0)$, $s_{CP}^{(i)}(1)$, ..., $s_{CP}^{(i)}(N-1)]^T$. The cyclic prefix added signal is then passed through the fast fading Rayleigh channel in the presence of AWGN. The signal at the receiver is given by:

$$\widetilde{y}^{(i)} = \widetilde{s_{CP}}^{(i)} \otimes h^{(i)} + \xi^{(i)} \qquad (2)$$

where
$$\widetilde{y}^{(i)} = [\widetilde{y}^{(i)}(-L_G + N), \widetilde{y}^{(i)}(-L_G + N + 1)..,$$
$$,\widetilde{y}^{(i)}((N-1)), \widetilde{y}^{(i)}(0), \widetilde{y}^{(i)}(1), ..., \widetilde{y}^{(i)}(N-1)]^T \text{ is the}$$
received i[th] OFDM symbol.

$h^{(i)} = [h^{(i)}(0), h^{(i)}(1), ..., (h^{(i)}(L-1)]^T$ is the channel impulse response vector of length L.

$\xi^{(i)} = [\xi^{(i)}(0), \xi^{(i)}(1), ... \xi^{(i)}(L-1)]^T$ is the AWGN vector.

$\otimes$ represents the convolution operation.

The cyclic prefix is removed for the cancellation of ISI to yield $y^{(i)}$. The time domain sequence $y^{(i)} = [y^{(i)}(0), y^{(i)}(1), ..., y^{(i)}(N-1)]^T$ is converted to the frequency domain by the operation of DFT as follows:

$$r^{(i)} = F^H y^{(i)} \qquad (3)$$

The signal is demapped after a channel estimation and equalization. Finally, the demapped signal is fed to a Turbo decoder to yield the output bits.

3. Anatomy of the Turbo Encoder & Decoder

3.1 Turbo Encoder

The encoder employed in this paper was of rate 1/3. Puncturing is also used to provide a variation of the code rate. The encoder consisted of two Recursive Systematic Convolutional (RSC) encoders concatenated via an interleaver, as shown in Fig. 2 [12]. A pseudo-random interleaver was considered in this study. The generator sequences, [1 1 0 1 1][1 1 0 0 1], [1 1 1][1 0 1] and [1 1 1 1][1 1 0 1], were used for the memory orders four, two and three, respectively, because of their better performance compared to other possible generator sequences [13]. The size of the interleaver used was equal to the number of bits per OFDM symbol.

3.1 Turbo Decoder

The iterative Turbo decoder for the encoder of rate 1/3 consisted of two component decoders, as shown in Fig. 2 [12]. The component decoders connected serially through the interleaver exchanges soft information between each other to improve the decoding performance. In this paper, three different decoding algorithms, i.e., MAP, Log-MAP and Max-Log-MAP are used. The performance and complexity comparison was also made between the decoding algorithms. The log likelihood ratio (LLR) for a received bit r_k is given by:
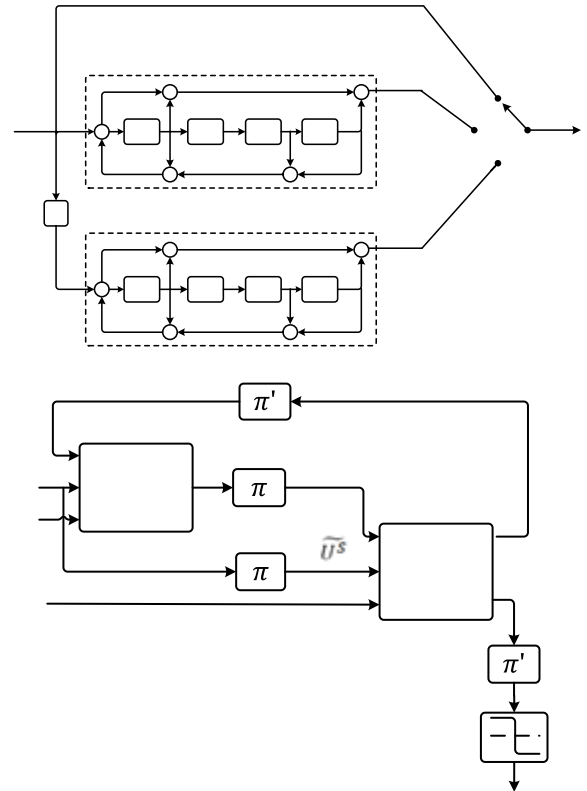

Fig. 2. (a) Parallel Concatenated Convolutional Codes (PCCC) Encoder, (b) Iterative Turbo Decoder.

$$LLR(r_k) = \ln\left(\frac{P(r_k=+1|y)}{P(r_k=-1|y)}\right) \qquad (4)$$

In the first iteration, the value of the LLR is 0 due to the assumption of equal probabilities of 1 and 0. In the iterative decoder, the extrinsic information of component decoder-1 is interleaved and then fed into component decoder-2. The extrinsic information of decoder-2 is de-interleaved and fed to component decoder-1. The iterative decoder exchanges soft information between the component decoders to improve its performance. In the final iteration, the LLR of component decoder-2 is deinterleaved and used for the hard decision.

4. Turbo Decoding Algorithms

4.1 MAP Decoding Algorithm

The operation of the MAP decoding algorithm proposed by Bahl *et al* is based on a minimization of the symbol error probability [14]. The MAP algorithm generates a soft output (a posteriori probability) using the received symbol sequence r. The LLR is given by:

$$\Lambda(c_t) = \ln\frac{P\{c_t=1|r\}}{P\{c_t=0|r\}} \qquad (5)$$

where $1 \le t \le T$ (T = length of the sequence r) and $P(*)$

represents the probability of *, and the hard estimate c_t is given by the following the condition:

$$c_t = \begin{cases} 1 & if \quad \Lambda(c_t) \geq 0 \\ 0 & otherwise \end{cases} \tag{6}$$

The soft information $\Lambda(c_t)$ of the component decoder-2 is used for the hard estimate, c_t, in the last iteration of the iterative decoding algorithm shown in Fig. 3, otherwise it is used by the next component decoder to improve the performance. The LLR defined in Eq. (5) can be re-written as:

$$\Lambda(c_t) = \ln \frac{\sum_{(l',l) \in B_t^1} \alpha_{t-1}(l') \gamma_t^1(l',l) \beta_t(l)}{\sum_{(l',l) \in B_t^0} \alpha_{t-1}(l') \gamma_t^0(l',l) \beta_t(l)} \tag{7}$$

where B_t^1 is the set containing the transitions $S_{t-1} = l' \rightarrow S_t = l$ for input bit1 and B_t^0 is the set containing the transitions $S_{t-1} = l' \rightarrow S_t = l$ for input bit 0, and $\alpha_{t-1}(l')$, $\beta_t(l)$ and $\gamma_t(l',l)$ are the forward metric, backward metric and transition metric, respectively. These metrics are given by:

$$\alpha_t(l) = \sum_{all\ l'} \alpha_{t-1}(l') \sum_{i \in (0,1)} \gamma_t^i(l',l) \ for\ t = 1,2,3,\dots,N \tag{8}$$

At $t = 0$, the boundary conditions, $\alpha_0(0) = 1$, and $\alpha_0(l) = 0$ for $l \neq 0$ are used.

$$\beta_t(l') = \sum_{all\ l'} \beta_{t+1}(l') \sum_{i \in (0,1)} \gamma_{t+1}^i(l,l') \ for\ t = N-1,\dots,1,0 \tag{9}$$

At $t = N$, the boundary conditions are $\beta_t(N) = 1$ and $\beta_t(N) = 0$ for $l \neq 0$.

$$\gamma_t^i(l',l) = \begin{cases} p_t(i)e^{-\left(\frac{\sum_{j=0}^{n-1}(r_{t,j}^i - x_{t,j}^i(l))^2}{2\sigma^2}\right)} & for\ (l,l') \in B_t^i \\ 0 & otherwise \end{cases} \tag{10}$$

where $x_{t,j}^i$ is the output of the encoder corresponding to input $c_t = i$ and the transition from $S_{t-1} = l' \rightarrow S_t = l$. $p_t(i)$ is the a priori probability of input $c_t = i$.

4.2 Log-MAP Decoding Algorithm

The large number of exponentiations and multiplications involved in the MAP algorithm make it undesirable for practical implementation. The MAP algorithm can be simplified using the log domain of forward metric $\overline{\alpha_t}(l)$, backward metric $\overline{\beta_t}(l)$ and transition metric $\overline{\gamma_t}^i(l',l)$. Eq. (10) can be re-written:

$$\overline{\gamma_t}^i(l',l) = ln\{\gamma_t^i(l',l)\} \tag{11}$$

Eq. (8) can be also written as:

$$\overline{\alpha_t}(l) = ln\{\alpha_t(l)\}$$
$$\overline{\alpha_t}(l) = ln \sum_{all\ l'} \sum_{i \in (0,1)} e^{\bar{a}_{t-1}(l') + \overline{\gamma_t}^i(l',l)} \tag{12}$$

The initial conditions are $\overline{\alpha_0}(0) = 0$ and $\overline{\alpha_0}(l) = -\infty$ for $l \neq 0$. Similarly, Eq. (9) can be written as:

$$\overline{\beta_t}(l) = ln\{\beta_t(l)\}$$
$$\overline{\beta_t}(l) = ln \sum_{all\ l'} \sum_{i \in (0,1)} e^{\overline{\beta}_{t+1}(l') + \overline{\gamma_t}^i(l,l')} \tag{13}$$

The initial conditions are $\overline{\beta_0}(N) = 0$ and $\overline{\beta_0}(l) = -\infty$ for $l \neq 0$.

The LLR is given by the following:

$$\Lambda(c_t) = ln \frac{\sum_{all\ l} e^{\bar{a}_{t-1}(l') + \overline{\gamma_t}^1(l',l) + \overline{\beta}_t(l)}}{\sum_{all\ l} e^{\bar{a}_{t-1}(l') + \overline{\gamma_t}^0(l',l) + \overline{\beta}_t(l)}} \tag{14}$$

The log-MAP algorithm uses the Jacobian algorithm, $\ln(e^x + e^y) = \max(x, y) + f_c(|x - y|)$, to simplify the MAP decoding algorithm. The correction function, f_c, can be implemented using a look-up table. The performance of the Log-MAP decoding algorithm is degraded slightly compared to the MAP algorithm because the correction term is implemented using lookup table that takes a limited number of values [15]. If the correction function is implemented precisely then the performance of the MAP and Log-MAP becomes the same. The correction function can also be implemented using a threshold detector [16].

The LLR becomes

$$\Lambda(c_t) = \max_l \{\bar{a}_{t-1}(l') + \overline{\gamma_t}^1(l',l) + \bar{\beta}_t(l)\} - \max_l\{\bar{a}_{t-1}(l') + \overline{\gamma_t}^0(l',l) + \bar{\beta}_t(l)\} + f_c \tag{15}$$

$\overline{\alpha_t}(l)$ and $\overline{\beta}(l)$ can be written as

$$\overline{\alpha_t}(l) = \max_{all\ l', i \in (0,1)} \{\bar{a}_{t-1}(l') + \overline{\gamma_t}^i(l',l)\} + f_c \tag{16}$$
$$\overline{\beta_t}(l) = \max_{all\ l', i \in (0,1)} \{\bar{\beta}_{t+1}(l') + \overline{\gamma}_{t+1}^i(l,l')\} + f_c \tag{17}$$

The multiplication operation in MAP algorithm is transformed to an addition operation in log-MAP decoding algorithm and exponentiation is also avoided.

4.3 Max-Log-MAP Decoding Algorithm

The computational complexity associated with Log-MAP algorithm is low compared to the MAP algorithm. On the other hand, to further reduce the complexity of the Log-MAP algorithm, the correction function that is implemented by using lookup table or threshold detector is ignored.

5. ICI Cancellation Algorithm

The one-dimensional frequency domain comb-type pilot aided channel estimation was used for an ICI cancellation because of its low computational complexity compared to the two dimensional channel estimation techniques and good tracking ability of rapid variations of the fast fading channel [17]. Fig. 3 shows the arrangement of pilots in a comb-type and block-type channel estimation strategy. According to [18], equispaced pilots are used to achieve the optimal performance. For equispaced pilots, the ratio of the number of subcarriers to the number of pilots per OFDM symbol should result in an integer. The channel impulse response at the pilot subcarriers was estimated using the Least Square (LS) Estimator. The LS estimate is given by the following [19]:

$$h_{ce} = y s^{-1} \qquad (18)$$

where y and s are the vectors containing the received and transmitted pilots, respectively. The channel frequency response at the data subcarriers was estimated using an interpolation technique in a comb-type channel estimation strategy.

This paper proposed an interpolation technique based on the reduction of the interpolation error and the noise inherent in the LS estimation. The LS estimator estimates the channel impulse response without considering the channel noise and its performance degrades. The channel impulse response is concentrated in the time domain [20]. The fading impulses of the channel lies at integer multiples of the system sampling rate, and there is no energy leakage for the sample spaced channels [21]. Fig. 4 shows the channel energy distribution in time and frequency domain. The channel energy for the sample spaced channel is contained in the first L taps in the time domain and distributed in the frequency domain over all subcarriers.

$$h[n] = \begin{cases} IFFT[h_t(K)], & n \leq L \\ 0 & , & L < n < N \end{cases} \qquad (19)$$

where $h_t(k)$ is the time domain channel impulse response at the kth sub carrier. The frequency domain comb-type channel estimation is used in this paper because of the distributed nature of the channel energy in the frequency domain. The distributed nature of the frequency domain comb-type pilots allows them to track the channel impulse variations effectively. The first L taps are the significant taps containing the channel impulse response. Therefore, it should be considered in an estimation of the channel impulse response time domain.

After estimating the channel frequency response at the pilot subcarriers, the interpolation technique was used to calculate the channel frequency response at the data subcarriers. If the estimated channel response is converted to the time domain, then the beyond the first L taps, the channel impulse is noise because the channel impulse response is concentrated in the first L taps [22]. The noise contained in the other taps must be cancelled out to improve the channel estimation performance. The
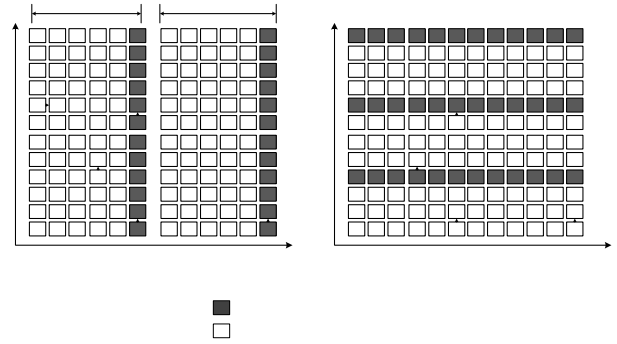

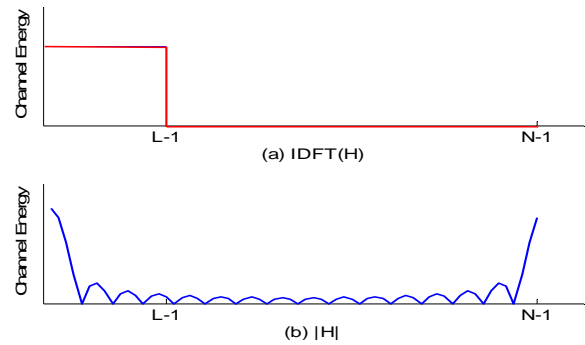**Fig. 3. Arrangement of the Pilots in Block-Type and Comb-Type Channel Estimation.**

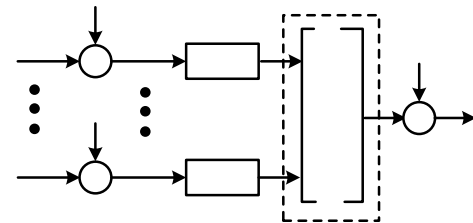**Fig. 4. Channel Energy Distribution in the time and Frequency domain.**

Fig. 5. Conceptual View of the proposed interpolation Technique.

proposed interpolation is based on minimizing the noise associated with a LS estimation, which enhances the performance of the LS estimator. Define $[M]_{p,n} = e^{j2\pi(p-1)(n-1)}/N$ for $n = 0, 1, 2, …, N-1$ and $p = 0, 1, 2, …, p-1$. The proposed interpolation technique consists of the following three steps:

(1) Multiply h_{ce} with the columns of the matrix, M, to yield the time domain vector, g, as shown in Fig. 5.

(2) Then multiply the vector g by the scalar, $1/P$.

(3) Finally, the frequency domain channel frequency response vector is calculated by the multiplication of M^H

with the scaled version of g .

The multiplication of M^H with the scaled version of the g yield h , whichcontains the estimated channel frequency response at all subcarriers. The effect of this multiplication suppresses noise and performs an estimation of the channel frequency response at all subcarriers. The performance of the proposed interpolation technique was compared with other one-dimensional interpolation techniques i.e. low pass, spline and linear interpolation.

6. Simulation Results & Analysis

The performance of OFDM system was evaluated for two different channel models through simulations performed on MATLAB. Table 1 lists the simulation parameters.

Channel Model A: The first channel model consists of L independent taps with a Gaussian distribution and zero mean. Constant and Exponential power delay profiles were used for a performance evaluation of the OFDM system model. The variance of each tap for exponential power delay profile is given by

$$\sigma^2_l(l) = e^{\frac{-l}{50}}, l = 0,1,2,\dots,L-1 \qquad (20)$$

Channel Model B: Six Stanford University Interim channel models are available. Three categories of terrain for the SUI channel models are A, B and C. Terrain A is for hilly areas with a moderate to heavy tree density and high path loss. Category B has either hilly or flat terrain. The tree density is moderate to heavy for the flat train and light for hilly terrain. Category C has flat terrain with light tree density. In this paper, SUI-6 channel model in the presence of AWGN is used for the performance evaluation of the proposed turbo coded OFDM system with a channel estimation. Table 2 lists the parameters of SUI-6. The normalization factor used in SUI-6 is -0.5683 dB. The

Doppler shifts in this paper is changed from [0.4 0.3 0.5] to [40 90 200] to make the channel more distorting.

The interpolation techniques used in this paper are the low pass, spline and the proposed interpolation technique. In the low pass interpolation (*interp* function in MATLAB), zeros are padded into the original sequence and the zero padded sequence is then passed through a low pass FIR filter [17]. The mean square error is minimized by a low pass interpolation between the ideal and interpolated points. In a spline cubic interpolation, a smooth and continuous polynomial fitted to the given data point is produced (*spline* function in MATLAB). The basic idea of drawing a smooth curve using a number of points is the basis of spline interpolation [23].

6.1 Effect of an Increase in the Channel Taps on the Performance of the LS estimator with interpolation Techniques

The performance of the LS estimator for channel model A was evaluated for a low pass interpolation, spline interpolation and proposed interpolation technique by varying the channel order. According to the authors of [24], the channel order depends on the environment, greater the diverse effects of the channel, greater will be the channel order and vice versa. They also reported that the value of channel order is twice for a bad urban environment compared to typical urban environment. The effect of an increase in the channel order on the performance of different interpolation techniques was studied, and is shown in Figs. 6 and 7. Figs. 6 and 7 show that the performance of the proposed interpolation technique remains stable while the performance of the other interpolation techniques degrades with increasing channel order. This adds to the robustness of the proposed interpolation technique.

Fig. 8 shows the performance of the LS estimator with different interpolation techniques for both constant and exponential power delay profiles for the channel order, L=18. The performance of the proposed interpolation technique is the same for both power delay profiles. On the other hand, the performance of the low pass and spline interpolation techniques is different for different power delay profiles. The performance degradation for higher SNRs in the case of constant power delay profile is more than for the exponential power delay profile. The reason for this improvement in performance is because of the exponential decaying nature of the channel energy for the exponential power delay profile. The higher channel taps in the case of the exponential power delay profile are less significant than the higher channel taps for a constant power delay profile. Therefore, the performance degradation for a constant power delay profile is higher than that of the exponential power delay profile. Table 3 lists the BER values for the uncoded OFDM with BPSK modulation scheme and the proposed interpolation technique for different channel orders. Table 3 shows that the BER performance is optimum for a channel order equal to the number of pilots per OFDM symbol. The proposed
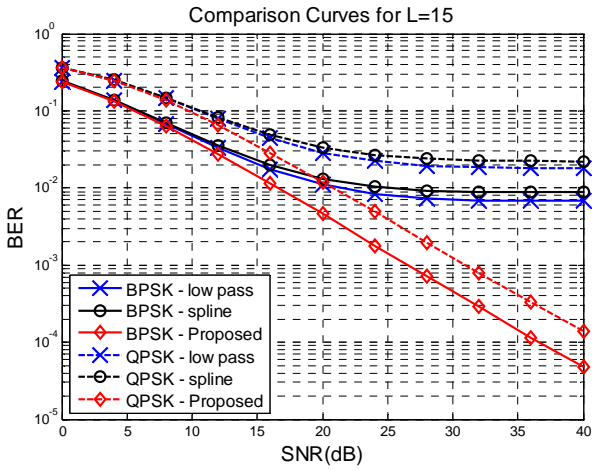
Table 1. Simulation Parameters.

Parameter	Specification
Number of Subcarriers, N	256
Size of IFFT	256
Cyclic Prefix Length	¼ i.e. 64
Channel Estimation	Comb-type
Pilot Ratio	1/8
Channel Model	SUI-6
Interpolation Techniques	Spline, Low Pass and Proposed

Table 2. SUI-6 Parameters Values.

	Tap 1	Tap 2	Tap 3	Units
Power	0	-10	-14	dB
Doppler	0.4	0.3	0.5	Hz
Delay	0	14	20	ms
Rician Factor, k	0	0	0	

Fig. 6. Performance Comparison of OFDM for the Rayleigh Fading Channel with a Constant Power Delay Profile for Channel order 15.
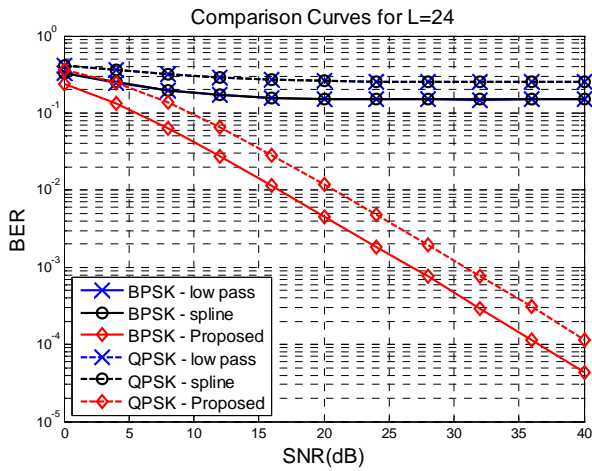

Fig. 7. Performance Comparison of OFDM for the Rayleigh Fading Channel with Constant Power Delay Profile for Channel order 24.
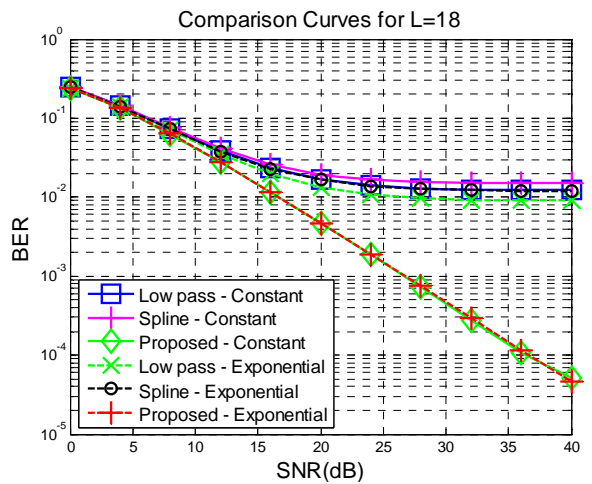

Fig. 8. Performance Comparison of OFDM for the Rayleigh Fading Channel for Channel order18.

Table 3. BER Comparison of the Proposed Interpolation in Uncoded OFDM for SNR=40 DB for Different Channel Orders.

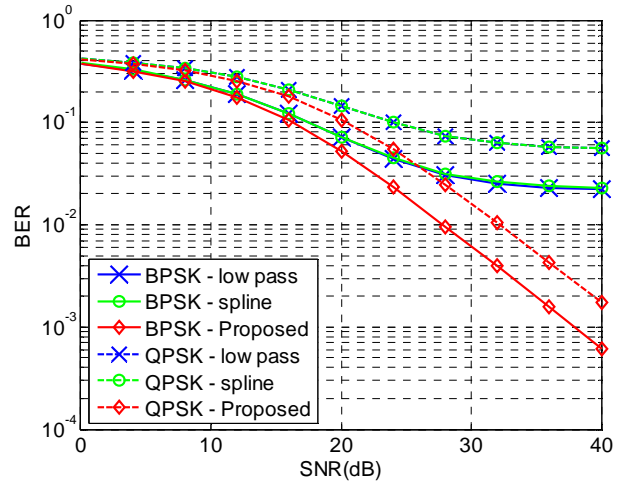| Channel Order	BER
15	4.792×10^{-5}
24	4.315×10^{-5}
32	4.2857×10^{-5}

Fig. 9. Performance of the uncoded OFDM with the BPSK and QPSK Modulation Schemes for different interpolation techniques.

interpolation technique cancels out the noise beyond the first P (number of pilots per OFDM symbol) taps in the time domain. When the channel order is less than P, the noise in the taps from $(L-1)^{th}$ tap to a $(P-1)^{th}$ Tap is not cancelled out by the proposed interpolation technique. Therefore, the performance of the proposed interpolation technique degrades slightly compared to the case when the channel order L and P are equal. The channel taps beyond the first L taps contain only noise in the time domain. The performance degradation of the Low pass and spline interpolation techniques is due to the noise inherent in the LS estimation and the interpolation error associated with them.

6.2 ICI Cancellation Performance Evaluation of the Proposed Scheme for Channel Model B

Fig. 9 shows the performance of uncoded OFDM for BPSK modulation scheme with a channel estimation for different interpolation techniques i.e. Proposed, Spline and Low pass interpolation technique. The performance of the channel estimation with the proposed interpolation technique was improved compared to the Spline and Low pass interpolation techniques due to the reduction of noise and interpolation error. The proposed interpolation technique considers the effect of noise, first converts the signal to a time domain to obtain the concentrated time domain channel impulse response, and the noise is then cancelled out and interpolation is performed to minimize

the interpolation error.

In [17, 25], it was shown through simulation results that the performance of one-dimensional interpolation techniques from the worst to best was in the following order for comb-type channel estimation for a LS estimator i.e. Linear, Second order, Time domain, Spline and Low pass. In this paper, the performance from worst to best was in the following order i.e. Spline, Low pass and Proposed interpolation technique. Therefore, the performance of the proposed interpolation technique is better than the Linear, Spline, Second order, Time domain and Low pass interpolation.

6.3 Error Correction Performance Evaluation of Turbo codes for Channel Model B

The legends MAP, Log-MAP, Max-Log-MAP and MO stand for MAP decoding algorithm, Log-MAP decoding algorithm, Max-Log-MAP decoding algorithm and memory order, respectively. For Figs. 10-14, the memory
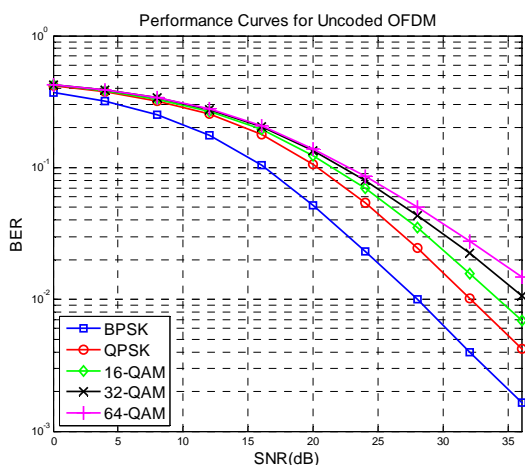

Fig. 12. Performance curves for MAP decoding algorithm with a different number of iterations in uncoded OFDM for BPSK modulation scheme.

Fig. 10. Performance of uncoded OFDM with the BPSK and QPSK Modulation Schemes for different interpolation techniques.

Fig. 13. Performance curves for Max-Log-MAP decoding algorithm with different number of iterations in uncoded OFDM for BPSK modulation scheme.
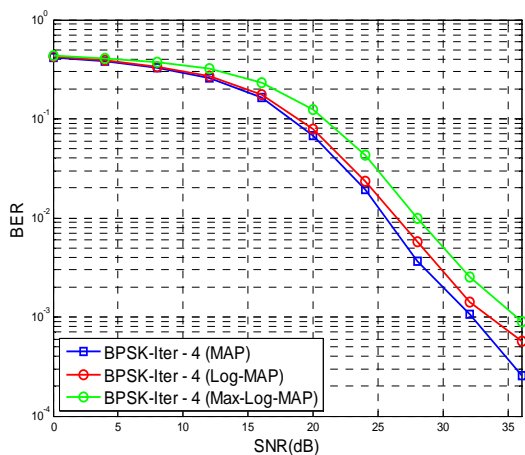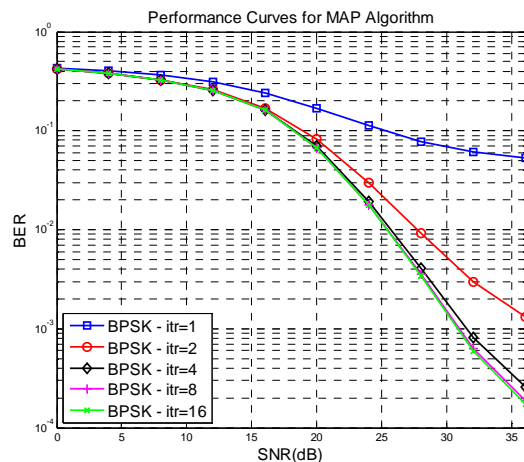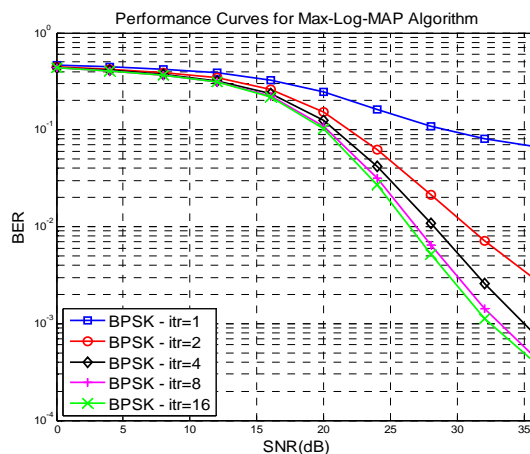

Fig. 11. Performance Comparison of the decoding algorithms with 4 iterations.
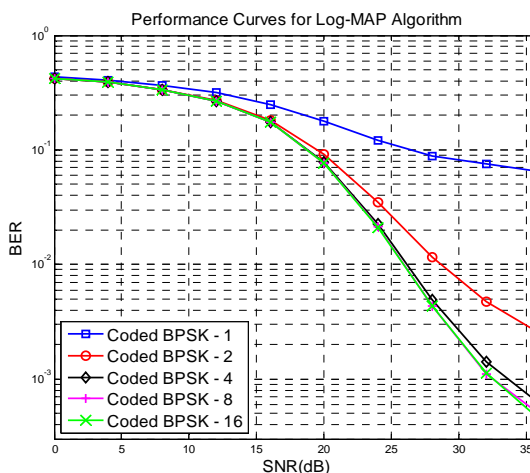

Fig. 14. Performance curves for Log-MAP decoding algorithm with a different number of iterations in uncoded OFDM for BPSK modulation scheme.

Table 4. Complexity Comparison of the Decoding Algorithms.

Decoding Algorithm	Additions	Multiplications	Maximization	Exponentiations	Lookups
MAP	$2 \times 2^k \times 2^v + 6$	$5 \times 2^k \times 2^v + 8$	0	$2 \times 2^k \times 2^v$	0
Log-MAP	$6 \times 2^k \times 2^v + 6$	$2^k \times 2^v$	$4 \times 2^v - 2$	0	2^v
Max-Log-MAP	$4 \times 2^k \times 2^v + 8$	$2 \times 2^k \times 2^v$	$4 \times 2^v - 2$	0	0

order 3 was used. In this subsection, the channel frequency response at the pilot subcarriers estimated using a LS estimator and channel frequency response at the data tones was estimated using the proposed interpolation technique. Fig. 8 shows the performance of the uncoded OFDM with different digital modulation schemes i.e. BPSK, QPSK, 16-QAM, 32-QAM and 64-QAM. Fig. 11 shows the performance of the turbo coded OFDM with BPSK modulation scheme for MAP, Log-MAP, Max-Log-MAP decoding algorithms for component decoders. The number of iterations used for the iterative turbo decoder for this section was 4.

The BER performance of the component decoders from the best to worst was in the following order, i.e., MAP, Log-MAP and Max-Log-MAP. Table 4 presents the results of a complexity comparison of the decoding algorithm. The number of operations for the decoding algorithm are represented for Convolutional code of rate k/n and memory order v. Table 4 clearly shows the high complexity associated with the MAP algorithm compared to the Log-MAP and Max-Log-MAP decoding algorithms. In the MAP decoding algorithm, all paths of the trellis are divided into two sets. One set was for input bit 0 and other was for input bit 1. The log-likelihood ratio was then calculated for each received symbol. In case of Max-Log-MAP and Log-MAP, only two paths per step is selected, one is the best path for input bit zero and the other is the best path for input bit 1. LLR is then computed for the two paths and yields the difference at the output. The only complexity of Log-MAP over Max-Log-MAP is the correction function. Trade-off is needed between the BER performance and complexity of the decoding algorithms.

Figs. 12-14 show the effect of an increase in the number of iterations of the iterative turbo decoder on the BER performance for MAP, Log-MAP and Max-Log-MAP decoding algorithms. In first iteration, the LLR is close to a zero mean but it deviates from the zero mean during the next two or three iterations in such a way that a further increase in the number of iterations just adds computational complexity to the system without significantly improving the performance of the system. This can explain the significant performance improvement during the first initial number of iterations compared to the later iterations.

Fig. 15 presents the effects of a variation of the memory order on the performance of decoding algorithms. The performance of the decoding algorithms improves with increasing memory order. The BER performance of Turbo codes depends on the free distance and effective free distance; both are related directly to the memory order. This explains performance improvement for an increase in memory order. On the other hand, an increase in memory
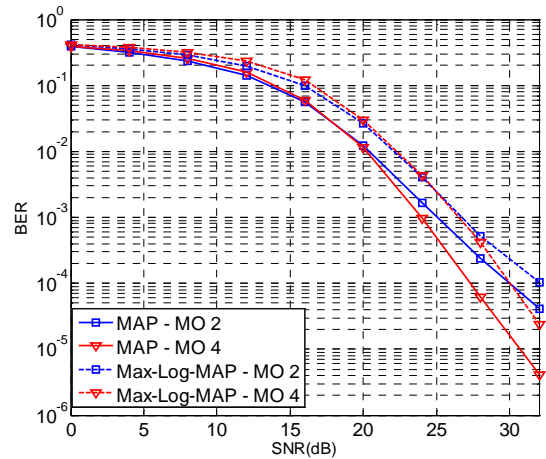

Fig. 15. Performance curves for Max-Log-MAP and MAP decoding algorithm with 4 iterations in uncoded OFDM for memory order 2 and 4 with BPSK modulation scheme.

order results in increased complexity, as indicated by Table 4. Therefore, some trade-off must be made between the performance and complexity.

7. Conclusions

An OFDM system model for joint error correction and ICI cancellation was proposed. The proposed model used a comb-type channel estimation to cancel out ICI. A robust interpolation technique with low computational complexity was proposed to estimate the channel frequency response at data subcarriers. The proposed interpolation outperformed other dimensional interpolation techniques, such as low pass and spline interpolation. The performance of the proposed interpolation technique remained acceptable for an increase in channel order while the performance degradation for the other dimensional interpolation techniques was so severe that they became useless for higher channel taps. In addition, Turbo codes were used to further improve the BER performance of the system. Performance and complexity comparisons were also made between the different decoding algorithms used for the component decoders in the iterative turbo decoder. MAP outperformed Log-MAP and Max-Log-MAP but at the expense of the high computational complexity. The effect of an increase in memory order on the performance of the turbo codes was also studied. The increase in memory order results in performance improvement but at the expense of the computational complexity.

References

[1] T.L. Willke, P. Tientrakool, N.F. Maxemchuk, "A survey of inter-vehicle communication protocols and their applications," *IEEE Communications Surveys & Tutorials*, vol.11, no.2, pp.3-20, Second Quarter 2009. Article (CrossRef Link)

[2] J. Armstrong, "Tutorial on optical OFDM," *2012 14th International Conference on Transparent Optical Networks (ICTON),* Coventry, UK, 2-5 July 2012 Article (CrossRef Link)

[3] A. B. Narasimhamurthy, M. K. Banavar and C. Tepedeleniogly, *OFDM Systems for Wireless Communications*, Morgan and Claypool publishers, 2010 Article (CrossRef Link)

[4] Z. Yang, W. Bai and Z. Liu, "A Decision-Aided Residual ISI Cancellation Algorithm for OFDM Systems," *2006 8th International Conference on Signal Processing*, Beijing, pp. 16-20, 2006 Article (CrossRef Link)

[5] P. Chayratsami, M.A. Wickert, "Novel mitigation techniques for OFDM in a Doppler spread channel," *2004 IEEE Radio and Wireless Conference,* pp. 395-398, 19-22 Sept. 2004 Article (CrossRef Link)

[6] Z. Jianhua, H. Rohling, Z. Ping, "Analysis of ICI cancellation scheme in OFDM systems with phase noise," *IEEE Transactions on Broadcasting,* vol.50, no.2, pp. 97- 106, June 2004 Article (CrossRef Link)

[7] A. Seyedi, G.J. Saulnier, "General ICI self-cancellation scheme for OFDM systems," *IEEE Transactions on Vehicular Technology,* vol.54, no.1, pp. 198- 210, Jan. 2005 Article (CrossRef Link)

[8] Wen-Sheng Hou, Bor-Sen Chen, "ICI cancellation for OFDM communication systems in time-varying multipath fading channels," *IEEE Transactions on Wireless Communications*, vol.4, no.5, pp. 2100-2110, Sept. 2005 Article (CrossRef Link)

[9] C. Berrou, A. Glavieux, P. Thitimajshima, Near Shannon limit error-correcting coding and decoding: turbo codes, *in the Proceedings of IEEE International Conference on Communications*, vol. 2 (Geneva), pp. 1064–1070. May 1993 Article (CrossRef Link)

[10] E. Yeo, B. Nikolic, and V. Anantharam, "Iterative Decoder Architectures", *IEEE Communication Magazine*, August2003, pp. 132-140. Article (CrossRef Link)

[11] G. Kiokes, G. Economakos, A. Amditis, N. K. Uzunoglu, "A Comparative Study of IEEE 802.11p Physical Layer Coding Schemes and FPGA Implementation for Inter Vehicle Communications" *Modern Traffic and Transportation Engineering Research,* Volume 2, Issue 2, pp. 95-102, April 2013. Article (CrossRef Link)

[12] B. Vucetic & J. Yuan, *Turbo Code, Principles and Applications. London*: Kluwer Academic Publishers, 2002 Article (CrossRef Link)

[13] S. Benedetto and G. Montorsi, "Design of Parallel Concatenated Convolutional Codes, " *IEEE trans. Communications*, vol. 44, no. 5, pp.591-600, May 1996 Article (CrossRef Link)

[14] L. R. Bahl, J. Cocke, F. Jelinek, and J. Raviv, "Optimal decoding oflinear codes for minimizing symbol error rate," IEEE Trans. Inform.Theory, vol. IT-20, pp. 284–287, 1974 Article (CrossRef Link)

[15] I.A. Chatzigeorgiou, M.R.D Rodrigues,. I.J. Wassell, R.A. Carrasco, "Comparison of Convolutional and Turbo Coding for Broadband FWA Systems," *IEEE Transactions on Broadcasting*, vol.53, no.2, pp.494-503, June 2007 Article (CrossRef Link)

[16] W.J. Gross, P.G. Gulak, "Simplified MAP algorithm suitable for implementation of turbo decoders," *Electronics Letters*, vol.34, no.16, pp.1577-1578, 6 Aug 1998 Article (CrossRef Link)

[17] Y. Shen and E. Martinez, "Channel Estimation in OFDM Systems," Free scale Semiconductor, AN3059Inc., 2006, Article (CrossRef Link)

[18] X. Cai, G.B. Giannakis, "Error probability minimizing pilots for OFDM with M-PSK modulation over Rayleigh-fading channels," *Vehicular Technology, IEEE Transactions on*, vol.53, no.1, pp. 146- 155, Jan. 2004, Article (CrossRef Link)

[19] W. Di-xiao, "On Comparison Of Pilot-Aided OFDM channel estimation algorithms," *Image Analysis and Signal Processing (IASP), 2011 International Conference on*, vol., no., pp.31-35, 21-23 Oct. 2011 Article (CrossRef Link)

[20] J. Ma, H. Yu, S. Liu, "The MMSE Channel Estimation Based on DFT for OFDM System," *5th International Conference on Wireless Communications, Networking and Mobile Computing, 2009. WiCom '09.*, pp.1,4, 24-26 Sept. 2009 Article (CrossRef Link)

[21] A. Chini, "Multicarrier Modulation in Frequency Selective Fading Channels. Ph.D. Thesis, Carleton University, Ottawa, Canada, 1994 Article (CrossRef Link)

[22] Y. Kang, K. Kim, H. Park, "Efficient DFT-based channel estimation for OFDM systems on multipath channels," *IET Communications*, vol.1, no.2, pp.197, 202, April 2007 Article (CrossRef Link)

[23] L. U. Khan, M. I Babar and Z. Sabir, "Robust modified MMSE estimator for comb-type channel estimation in OFDM systems," *2013 15th International Conference on Advanced Communication Technology (ICACT)*, PyeongChang , Korea, pp.924-928, 27-30 Jan. 2013. Article (CrossRef Link)

[24] COST 207 TD(86)51-REV 3 (WG1), 'Proposal on channel transfer functions to be used in GSM tests late 1986', Standard, 1986 Article (CrossRef Link)

[25] S. Coleri, M. Ergen, A. Puri, A.Bahai, "Channel estimation techniques based on pilot arrangement in OFDM systems," *IEEE Transactions on Broadcasting*, vol.48, no.3, pp.223,229, Sep 2002. Article (CrossRef Link)

Latif Ullah Khan is currently working as a Lecturer at Electrical Engineering department, University of Engineering & technology Peshawar, Pakistan. He received his B.Sc degree in Electrical Engineering from the University of Engineering &Technology Peshawar, Pakistan and is currently pursuing his M.Sc degree in Electrical Engineering from the same University. He is a member of IEEE USA and had the honor to win the best paper award in the 15th IEEE International Conference on Advanced Communication Technology, (ICACT-2013) in South Korea. His research interests include channel estimations in OFDM, channel coding, intelligent system design and routing protocols in Mobile Ad-hoc Networks (MANETs).

Muhammad Irfan Khattak completed his BSc in Electrical Engineering from NWFP University of Engineering and Technology Peshawar, Pakistan in 2004 and his PhD from Loughborough University, UK in 2010. Currently, he is Assistant Professor at NWFP University of Engineering and Technology, Pakistan.

Naeem Khan graduated from the University of Engineering & Technology, Peshawar, Pakistan in 2003, and received the M.Sc. in electrical power engineering from the same institute in 2007, and obtained the Ph.D. degree in control and communication system from the University of Leicester, Leicester, UK in 2012. Currently, he is Assistant Professor at NWFP University of Engineering and Technology, Bannu Campus, Pakistan. He has published various refereed journal and reputed conference papers. His research interests include robust control, state estimation under intermittent observations, and linear parameter varying systems.

Atif Sardar Khan did his B.Sc in Electrical Engineering from University of Engineering & Technology, Peshawar, Pakistan and currently pursuing his M.Sc in Electrical Engineering from the same university. Currently he is serving as a lecturer at Computer system engineering department, University of Engineering & Technology Peshawar. His research interests include Channel Coding, Channel Estimation and PAPR reduction in OFDM.

Muhammad Shafi completed his Bachelor in Computer System Engineering from Ghulam Ishaq Khan Institute of Engineering Sciences and Technology, Pakistan in 2005 and his PhD from the Department of Computer Science, Loughborough University, UK in 2010. Currently he is assistant professor at NWFP University of Engineering and Technology, Pakistan.